Interface focus

J. R. Soc. Interface (2010) **7**, S15–S26
doi:10.1098/rsif.2009.0329.focus
Published online 21 October 2009

Nanoparticle interaction with model lung surfactant monolayers

Rakesh Kumar Harishchandra, Mohammed Saleem[†] and Hans-Joachim Galla*

Institute of Biochemistry, Westfälische Wilhelms Universität, Wilhelm Klemm Street 2, 48149 Münster, Germany

One of the most important functions of the lung surfactant monolayer is to form the first line of defence against inhaled aerosols such as nanoparticles (NPs), which remains largely unexplored. We report here, for the first time, the interaction of polyorganosiloxane NPs (AmorSil20: 22 nm in diameter) with lipid monolayers characteristic of alveolar surfactant. To enable a better understanding, the current knowledge about an established model surface film that mimics the surface properties of the lung is reviewed and major results originating from our group are summarized. The pure lipid components dipalmitoylphosphatidylcholine and dipalmitoylphosphatidylglycerol have been used to study the biophysical behaviour of their monolayer films spread at the air–water interface in the presence of NPs. Film balance measurements combined with video-enhanced fluorescence microscopy have been used to investigate the formation of domain structures and the changes in the surface pattern induced by NPs. We are able to show that NPs are incorporated into lipid monolayers with a clear preference for defect structures at the fluid–crystalline interface leading to a considerable monolayer expansion and fluidization. NPs remain at the air–water interface probably by coating themselves with lipids in a self-assembly process, thereby exhibiting hydrophobic surface properties. We also show that the domain structure in lipid layers containing surfactant protein C, which is potentially responsible for the proper functioning of surfactant material, is considerably affected by NPs.

Keywords: lung surfactant; lipid monolayers; film balance; nanoparticles; domain structures

1. INTRODUCTION

The pulmonary surfactant of vertebrate lungs is a highly surface active complex lipid–protein monolayer lining the air–liquid interface of the alveoli. Its presence is an important prerequisite for the proper functioning of the lungs, facilitating gaseous exchange. It is crucial for continuous breathing as it prevents alveolar collapse by reducing the surface tension at the air–water interface during end-expiration, thereby minimizing the work of breathing (Goerke 1974; Schurch *et al.* 1976; Hills 1990). In addition, it acts as a first line of defence against inhaled particles and microbes, thus protecting the lungs from injuries and infections (Creuwels *et al.* 1997). The proteolipidic material is synthesized as large, tightly packed concentric layers of storage granules (lamellar bodies) by type II pneumocytes, one of the cell types forming the alveolar epithelium. The secretion of the lamellar bodies into the hypophase follows a highly regulated exocytic pathway. Subsequent transition from storage form to functional surface film involves unravelling of the lamellae and adsorption of lipids to form an interfacial surfactant film or insertion of lipids into an existing surfactant monolayer (Dietl & Haller 2005; Perez-Gil 2008). The lack or malfunction in secretion and adsorption of these essential materials leads to an acute respiratory dysfunction. In fact, the neonatal respiratory distress syndrome is one of the main reasons for the death of most premature births. It is also a major cause of morbidity and mortality in preterm infants (Creuwels *et al.* 1997; Clements & Avery 1998; Griese 1999).

The analysis of materials from bronchoalveolar lavage of animal lungs has been used to study the composition of surfactant materials. In general, pulmonary surfactant comprises primarily lipids (approx. 85–90%), especially phosphatidylcholines (PCs), phosphatidylglycerols (PGs) and other unsaturated phospholipids, in addition to small amounts of fatty acids, cholesterol and proteins (8–10%) (Yu *et al.* 1983; Goerke 1998; Veldhuizen *et al.* 1998). The di-saturated and zwitterionic dipalmitoylphosphatidylcholine (DPPC) is the predominant phospholipid, and is mainly responsible for low surface tension and withstanding high surface pressure (Watkins 1968; Schurch *et al.* 1976). However, when used alone, it functions poorly because it forms a rigid structure, thereby

*Author for correspondence (gallah@uni-muenster.de).
[†]Present address: Physical Chemistry Unit, Institute Curie, 75005 Paris, France.

One contribution to a Theme Supplement 'NanoBioInterface: crossing borders'.

Received 31 July 2009
Accepted 23 September 2009

re-spreading and adsorbing slowly at the interface. In contrast, anionic PGs and unsaturated phospholipids are good fluidizers, which is most relevant for monolayer respreading and enhancement of lipid adsorption from vesicles. Besides phospholipids, four surfactant-specific proteins have been found to be associated with lung surfactant (LS); these are designated as surfactant protein A (SP-A), SP-B, SP-C and SP-D. SP-A and SP-D, large hydrophilic proteins, are involved in the regulation of surfactant homeostasis and alveolar defence (Reid 1998; Crouch & Wright 2001; Kishore *et al.* 2006). On the other hand, SP-B and SP-C are very small and highly hydrophobic polypeptides mainly involved in the surface activity of LS. Each of them accounts for not more than 1–1.5% of total surfactant weight; despite their low abundance, they play a pivotal role in the formation and stabilization of pulmonary surfactant film.

The lipid–peptide components in the surfactant monolayer interact with and complement each other during compression and expansion of the breathing cycle. According to the so-called 'squeeze out' theory, during compression fluidizing lipids and surfactant proteins are believed to be selectively squeezed out, leaving behind a monolayer, at the interface, enriched in lipids (mainly DPPC) that promotes low surface tension (Watkins 1968; Bangham *et al.* 1979; Pastrana-Rios *et al.* 1994). The excluded substances form the multi-lamellar structures just beneath the surfactant monolayer and quickly re-spread on expansion. These topographic structures have been detected and visualized by means of scanning force microscopy (SFM) and transmission electron microscopy (Amrein *et al.* 1997; Galla *et al.* 1998; Krol *et al.* 2000*a*,*b*). The studies revealed that SP-B and SP-C are absolutely essential for the formation of the multi-layer structures which are necessary to prevent alveolar collapse as well as adsorption of materials onto the interface, thus facilitating the normal breathing process (Oosterlaken-Dijksterhuis *et al.* 1991*a*,*b*; Ross *et al.* 2002).

Owing to the highly complex and dynamic nature of the LS systems, it is very difficult to study the biophysical interactions in a real time course. Extensive research has been carried out in recent decades in investigating the composition of surfactant and thereby proposing various molecular model systems. Langmuir–Blodgett monolayers provide a very good system to study and understand the physiological behaviour of pulmonary surfactant at the air–liquid interface *in vitro*. The studies were performed using the LS model systems composed of a monolayer containing the neutral lipid DPPC and the negatively charged dipalmitoylphophatidylglycerol (DPPG) along with surfactant-specific proteins SP-B and/or SP-C. Thus, a well-defined and highly reproducible surfactant model system has been developed, which closely mimics the behaviour of natural surfactant (von Nahmen *et al.* 1997; Krol *et al.* 2000*a*).

With the advent of nanosciences, the use of nanotechnology has become widespread in various scientific fields from cosmetics and electronics to medicines, particularly in diagnosis and drug delivery (Mazzola 2003; Salata 2004). Nanomaterials can be defined as particles with at least one dimension measuring 100 nm or less, which includes nanoparticles (NPs), nanotubes, nanocomposites, etc. Owing to their nanosize, these particles confer unique physico-chemical properties that are most essential in making engineered NPs, and such properties make them very attractive in commercial and medicinal developments. The increasing use of nanotechnology has led to the release of nanomaterials in the environment and has raised questions about potential health risks (Nel *et al.* 2006). In contrast to many efforts aimed at exploiting the desirable properties of NPs, there have been limited attempts to evaluate potentially undesirable effects of these particles when released in the environment or administered intentionally for medicinal purposes (De Jong & Borm 2008; Yang *et al.* 2008). The effect these particles would have on human health is still the topic of debate. The pulmonary route of administration is of increasing interest, because of its non-invasive mode of uptake. This route can be used not only for the treatment of lung diseases but also for quick and efficacious systemic delivery of a drug (Sung *et al.* 2007). Also, besides the skin, the respiratory system is an important portal of entry as well as a target organ for NPs (Hoet *et al.* 2004). It is well known that the lungs are easily exposed to particles present in the atmosphere, unavoidably making contact with the inner surface of the alveolus. This inner surface of the alveoli, containing the LS monolayer, is the first barrier that any foreign substance encounters in order to enter the circulatory system. Knowing this fact and also the importance of the surfactant monolayer, which is crucial for proper breathing, means that it is imperative to investigate whether there is any destabilizing effect on interaction with nano-sized particles (NSPs). It has been shown that NSPs interact with LS and are thought to have an influence on physiological aspects such as surfactant metabolism, particle clearance and NP-induced toxicity (Schleh & Hohlfeld 2009).

To date, there have not been many studies that have investigated the effect of NPs on pulmonary surfactant model systems using biophysical techniques. In addition, the surfactant model used for the studies contained mainly lipids, giving the basic and essential information required (Stuart *et al.* 2006; Ku *et al.* 2008) to aid further in understanding the effect of the particles on complex LS model systems containing the lipid–protein monolayer. More important to LS function, a refined DPPC monolayer cannot mimic the proper activity of the LS monolayer in terms of re-spreadability, reversible hysteresis upon cycling and incorporation of new material at the interface. In addition, a study has been carried out investigating the effect of gold NPs on lipid/SP-B mixtures and showed that the lipid and protein would interact with the NPs, thereby inhibiting surfactant functioning (Bakshi *et al.* 2008). The previous studies have mainly investigated the effect of NPs on the phase behaviour of a lipid system. It would be interesting to visualize NP–surfactant monolayer interactions using microscopic techniques as well as characterization of the NP influence on two- and three-dimensional organization of the surfactant model system.

In the present study, we first describe the surfactant model system that was established by our group that mimics the natural LS system *in vitro*. The various techniques used for analysis and optimization are also described. In addition, we present the first results of the NP–surfactant model system interaction that gives a basic insight into and further assists in understanding the possible mechanism by which NPs interact with and pass through the surfactant monolayer.

2. MATERIAL AND METHODS

2.1. Materials

The lipids used in this study, namely 1,2-dipalmitoyl-*sn*-glycero-3-phosphocholine (DPPC) and 1,2-dipalmitoyl-*sn*-glycero-3-phosphoglycerol (DPPG) were purchased from Avanti Polar Lipids Inc. (Alabaster, AL, USA). 2-(4,4-Difluoro-5-methyl-4-bora-3a,4a-diaza-*s*-indacene-3-dodecanoyl)-1-hexadecanoyl-*sn*-glycero-3-phosphocholine (BODIPY-PC) was obtained from Molecular Probes (Eugene, OR, USA). All lipids were used without further purification. Chloroform and methanol were of high-pressure liquid chromatography grade and purchased from Roth (Karlsruhe, Germany). Water was purified and deionized by a multi-cartridge system (MilliPore, Billerica, MA, USA) and had a resistivity greater than 18 MΩ m. SP-C was isolated from porcine bronchoalveolar lavage fluid by the butanol extraction method (Haagsman *et al.* 1987; Taneva *et al.* 1998). The concentration of peptide was estimated by fluorescamine assay. Lipids and peptides were dissolved in chloroform/methanol solution (1 : 1, v/v).

2.2. Sample preparation

Polyorganosiloxane (AmorSil20) NPs, which consist of a core-shell NP with polyorganosiloxane nanospheres and polydimethylsiloxane (PDMS) core, and have a non-functional surface and are hydrophobic in nature (Roos *et al.* 1999) (kindly provided by Dr Michael Maskos, Institute for Physical Chemistry, University of Mainz), were dissolved in chloroform to get a concentration of $10\ \mathrm{mg\ ml^{-1}}$ corresponding to 1.93×10^{15} particles $\mathrm{ml^{-1}}$. The sample solutions were prepared by mixing NPs with lipid solution ($1\ \mathrm{mg\ ml^{-1}}$) corresponding to 500 : 1, 100 : 1, 10 : 1, 5 : 1, 1 : 1 v/v lipid/NP ratios.

Both the lipids and the NPs were in chloroform/methanol solution prior to injection onto the buffer surface. Spraying of NPs in order to mimic the natural condition of inhalation and adsorption onto the surfactant monolayer is technically challenging. In particular, controlled stoichiometry of NPs is important for the experiment as well as for interpretation and such an adsorption onto the monolayer is extremely difficult to attain by means of spraying. Thus, we adopted the conventional method of injecting the sample over the subphase in solution form. Such an approach, however, should not interfere with ideal lipid/particle interactions as the solvent quickly evaporates.

2.3. Surface pressure–area isotherms

All the film balance experiments were performed on an analytical Wilhelmy film balance (Riegler and Kirstein, Mainz, Germany) with an operational area of $144\ \mathrm{cm^2}$. All surface pressure–area measurements were performed on pure water, pH 5.6, 20°C. The spread monolayers were composed of DPPC, DPPG or DPPC/DPPG (4 : 1, mol ratio) and supplemented with various concentrations of NPs. The lipid/NP mixtures were prepared in a chloroform/methanol solution (1 : 1, v/v) and spread onto the subphase. After an equilibration time of 10–15 min the monolayers were compressed at a rate of $2.9\ \mathrm{cm^2\ min^{-1}}$.

2.4. Fluorescence light microscopy

Domain structures of lipid/NP samples doped with 0.5 mol% BODIPY-PC were visualized by means of an epifluorescence microscope (Olympus STM5-MJS, Olympus, Hamburg, Germany) equipped with an *xy*-stage and connected to a CCD camera (Hamamatsu, Herrsching, Germany). The images were captured at desired surface pressures by stopping the barrier. All the measurements were performed on a subphase containing pure water, pH 5.6, at 20°C.

2.5. Atomic force microscopy

Atomic force microscopy (AFM) images of the Langmuir–Blodgett (LB) films transferred onto mica sheets (for LB transfer, see Krol *et al.* (2000*a*)) were obtained under ambient conditions (20°C) using a Dimension 3000 scanning force microscope with a Nanoscope IIIa controller from Digital Instruments (Santa Barbara, CA, USA) operating in contact mode. Silicon nitride tips (Budget Sensors, Sofia, Bulgaria) with a spring constant of $40\ \mathrm{N\ m^{-1}}$ and a resonance frequency of 300 ± 100 kHz were used. The image processing and a detailed section height analysis of the images were performed using WsXM/Nanoscope SFM software (Horcas *et al.* 2007).

3. RESULTS AND DISCUSSION

3.1. State-of-the-art review of the surfactant reservoir hypothesis

Figure 1 presents the actual view of the LS under compression as seen in an electron micrograph compared with a schematic diagram. Surface-confined three-dimensional protrusions are found attached to the surface monolayer forming stacks of protein (SP-C and SP-B) stabilized bilayers. Such multilayer stacks have also been observed *in vivo* (Schurch *et al.* 1995).

Lipid–peptide monolayers at the air–water interface can be investigated using Langmuir film balance measurements. The biophysical techniques yielding such a defined molecular picture will be outlined shortly in a subsequent section. A basic technique used to study the phase behaviour of monolayers is the so-called Langmuir film balance. Amphiphilic molecules are spread on an aqueous subphase, forming a monolayer. Upon compression, the decrease in molecular

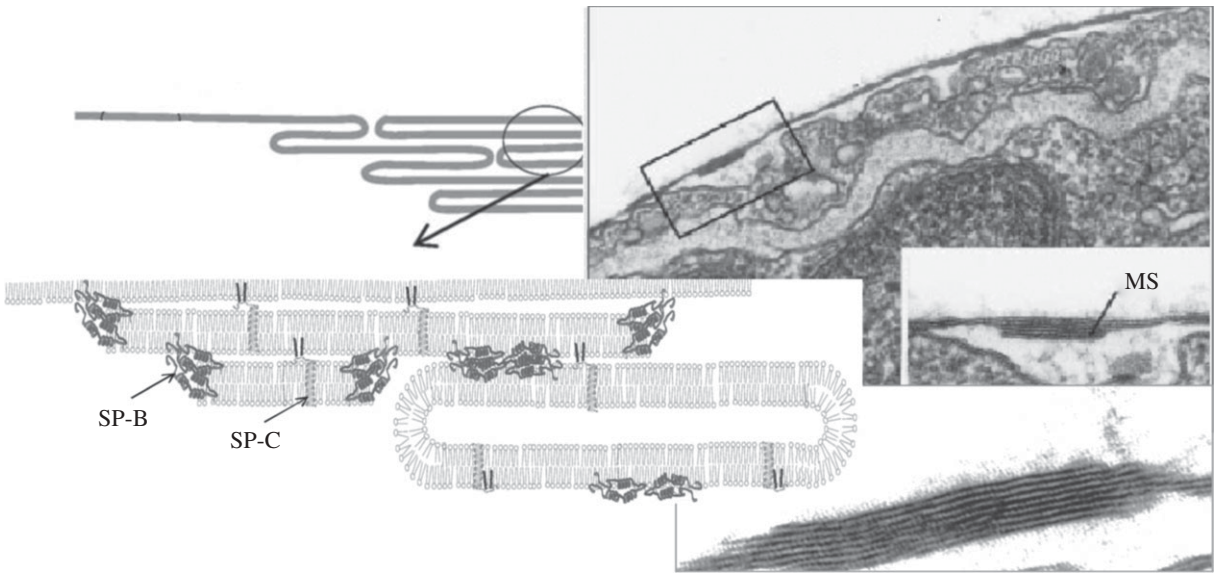

Figure 1. Overview on the model surfactant system comparing a schematic figure with an electron micrograph showing the multi-lamellar protrusion (Schurch *et al.* 1995; Galla *et al.* 1998; Perez-Gil 2008).

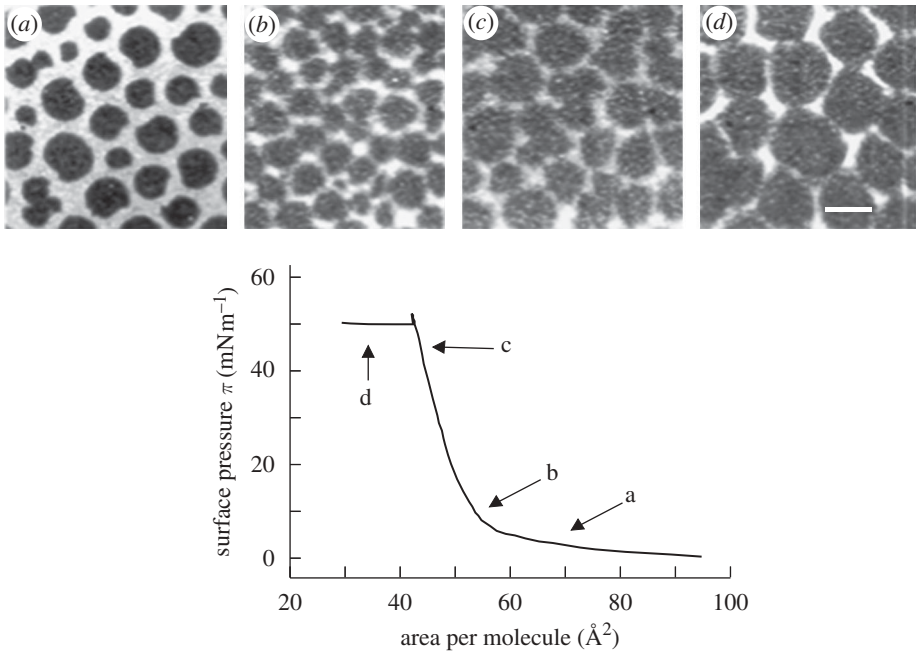

Figure 2. A characteristic surface pressure–area (π–A) isotherm of a monolayer containing DPPC/DPPG/SPC (80 : 20 : 0.4 mol ratio). The arrows point to the different surface pressure regions at which the fluorescent images (a–d) were taken. Scale bar, 10 μm.

area (Å^2) is accompanied by an increase in lateral surface pressure π (figure 2). In lipid monolayers containing surfactant proteins C or B, the increase in surface pressure continues until a plateau is reached. On further compression, the surface pressure is not changed under compression, giving rise to the assumption that the molecules are squeezed out of the plane into the subphase forming multilayer structures (figure 1). The structural lateral organization of the obtained film may be further inspected by video-enhanced fluorescence microscopy along the surface pressure–area curve (π–A). Using a fluorescent dye that is soluble only in the fluid phase, the analysis of the shape of the resulting domain structure provides extremely valuable information to understand the phase behavioural changes of the components in the monolayer. Figure 2 shows that further bright areas appear under compression along the plateau, supporting the finding of fluidized multilayer structures surrounding the condensed domains within the monolayer at reduced surface area. Furthermore, transferring the monolayers onto solid supports by the Langmuir–Blodgett technique, maintaining the native structures formed at the air–water interface, allows topological inspection by atomic force microscopy (figure 3*a*). The overall pattern is resolved at a

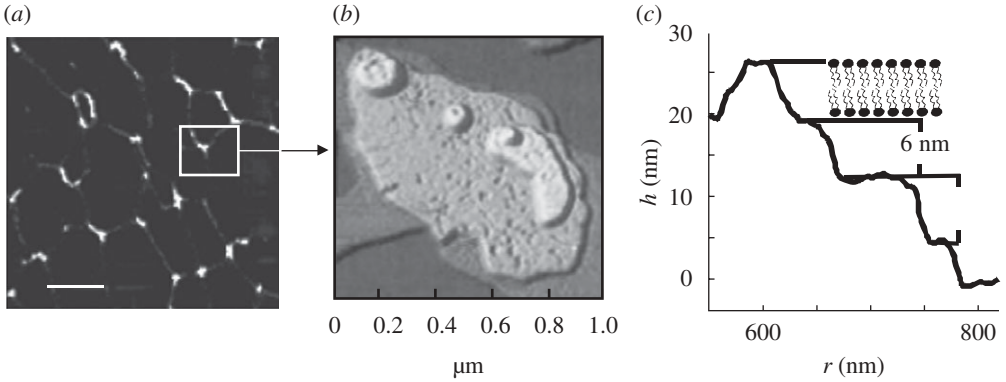

Figure 3. AFM topography images of monolayers consisting of DPPC/DPPG/SP-C (0.4 mol % peptide). (*a*) AFM images with scan size 10 × 10 μm^2 (scale bar, 2 μm); (*b*) the fine structure of the film shown as different layers in a pseudo-three-dimensional view (von Nahmen *et al.* 1997); (*c*) height profile of surface-confined multi-lamellar displaying the bilayer stacks of height corresponding to approximately 6 nm. Image analysis by WsXM/Nanoscope software revealed the height profile of the regions falling on the line scan as shown.

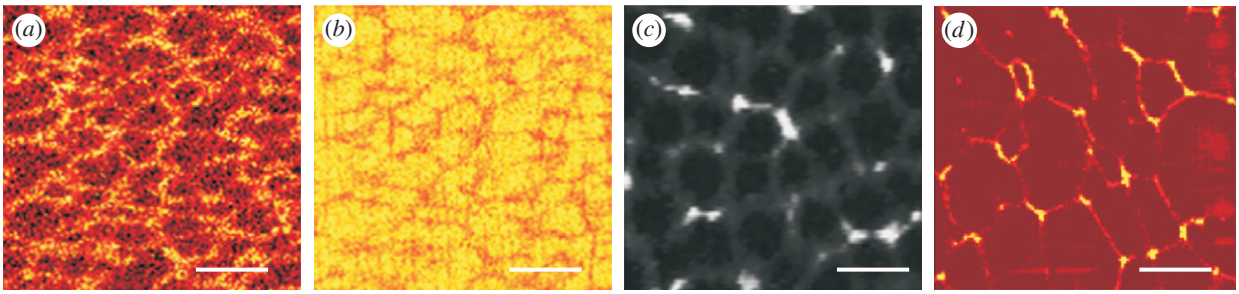

Figure 4. Comparative correlation of a surface view of a monolayer by various techniques. SIMS image showing the secondary ion intensity corresponding to (*a*) SP-C (CH_4N) and (*b*) DPPC (C_3H_8N), showing phase separation. The bright-coloured regions (yellow) denote high-intensity count, whereas the darker regions (brown) denote low-intensity count. (*c*) Fluorescence microscopy image showing the condensed and fluid phase and (*d*) atomic force microscopy image showing the topology of the phase-separated regions. Scale bars, (*a*,*b*) 30 μm, (*c*) 10 μm and (*d*) 2 μm.

molecular level and we could visualize the postulated three-dimensional structures in detail (figure 3*b*). The formation of bilayer stacks with a step height of 6 nm nicely fits to a bilayer including the surface water (figure 3*c*) (Amrein *et al.* 1997; von Nahmen *et al.* 1997; Krol *et al.* 2000*a*,*b*; Malcharek *et al.* 2005).

Moreover, we were able to analyse the chemical composition by time-of-flight secondary ion mass spectrometry (TOF-SIMS) (Breitenstein *et al.* 2006; Seifert *et al.* 2007; Saleem *et al.* 2008), which is a powerful technique for high-resolution surface, interface and thin film analysis that enables label-free detection of individual components of a monolayer, transferred to a solid support. TOF-SIMS involves rastering of a highly energetic electrically focused primary ion beam across the sample inducing a collision cascade that eventually leads to the release of charged molecules, which are secondary ion fragments (Benninghoven 1994). Further, the emitted fragment ions are accelerated by an electric field in the time-of-flight analyser, leading to the separation and detection of the ions differing in their mass-to-charge ratios (m/z). Thus, a chemical map can be generated showing the lateral distribution of chemical components down to a resolution of 80 nm. The TOF-SIMS chemical pattern (figure 4*a*,*b*) is identical to the fluorescence pattern (fluidity) (figure 4*c*) and the pattern observed by AFM (topology) (figure 4*d*). Analysing the fragments coming from the different

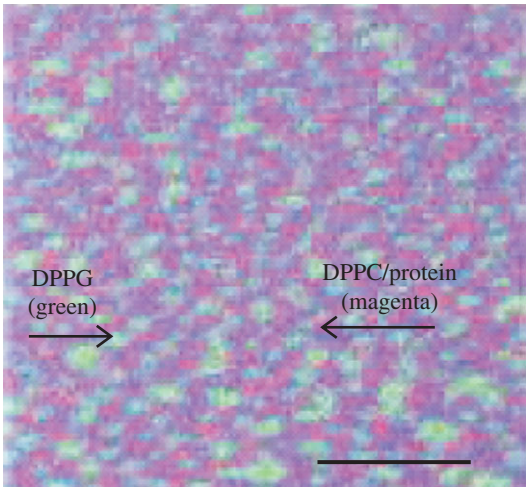

Figure 5. A three-colour overlay image showing the lateral co-localization of lipid–protein in the surfactant model system. This sum image is generated by superimposition of the mass resolved TOF-SIMS images of individual components of a monolayer, with positively charged secondary ions resulting from DPPC (m/z184, blue), *d62DPPG* (m/z 50, green) and protein (m/z84, red) (not shown). The superimposed primary colours fuse to give the final colour that denotes the co-localization. In the above example, DPPC (blue) and protein (red) are found to be mapped at the same regions, thus giving rise to a magenta-coloured network that comprises exclusive DPPG (green) domains. Scale bar, 30 μm.

components of the monolayer (different lipids and surfactant protein), we were able to impose a chemical map of the surface layer (figure 4*a*,*b*) where the superposition gives information about the molecular interactions (figure 5). The latter gives an example where the positively charged mimetic peptide KL4 is co-localized with the neutral DPPC, although an interaction with the negatively charged DPPG was expected (Saleem *et al.* 2008). Similar observations were also made with SP-B (Breitenstein *et al.* 2006; Seifert *et al.* 2007; Saleem *et al.* 2009). The co-localization of SP-B or KL_4 with either DPPC or DPPG, however, depends on the fluidity of the domain, which in turn depends on the subphase ionic conditions whereby apparent reversal of protein co-localization with DPPG was found (Saleem *et al.* 2009).

3.2. Film balance measurements of the effect of nanoparticles on lipid monolayers

In order to investigate the effect of NPs on the LS model system, we first systematically analysed the concentration-dependent effect of NPs on the individual mixtures of DPPC, DPPG and DPPC/DPPG (4 : 1 mol ratio).

3.2.1. Film balance studies of pure nanoparticles. The isotherms obtained for pure NPs and lipid monolayers containing AmorSil20 NPs are presented in figure 6*a*. Even in the absence of lipids, the organosiloxane NPs form a monolayer film and remain on the surface during compression up to a maximum surface pressure of approximately 21 mN m^{-1}. On expansion, the particles do not re-spread; rather, the isotherms show a sharp fall in the surface pressure, which is indicative of a large amount of NPs escaping/disappearing into the subphase. Thus, it is clear that NPs can form a monolayer by spreading themselves at air–water interfaces probably because of the strong surface tension of the water.

3.2.2. Effect of nanoparticles on the isotherms of the dipalmitoylphosphatidylcholine monolayers. NPs were mixed with the lipid solutions in varying ratios used for surface pressure isotherm measurements. The obtained results for DPPC, shown in figure 6*b*, exhibit a clear and well-known cooperative phase transition from the liquid expanded (le) to the liquid condensed (lc) state at 7 mN m^{-1} with a corresponding area of approximately 20 $Å^2$. Increasing amounts of NPs lead to the disappearance of this DPPC-specific transition region, slightly shifting the isotherms to larger molecular areas. At low NP concentration, there is not much effect on the phase transition region but a slight expansion can be observed. As the concentration is increased, the phase co-existence plateau is disturbed, eventually becomes less horizontal and finally vanishes. Interestingly, a small shoulder is noticed at the surface pressure of approximately 25 mN m^{-1}. Such a 'kink' can be attributed to the squeeze out of the material into the subphase. This squeeze out is clearly visble at the 1 : 1 ratio, where the isotherm crosses that of the pure lipid and reaches areas down to 10 Å/molecule, which is far beyond the area occupied by one lipid molecule.

3.2.3. Effect of nanoparticles on the isotherms of the dipalmitoylphophatidylglycerol monolayer. Figure 6*c* shows the effect of NPs on the phase behaviour of DPPG. At low NP concentrations, only a minor effect can be observed on the overall shape of the DPPG isotherm. The isotherms, however, exhibit a significant expansion when compared with DPPC/NPs monolayers. The shift of the isotherm to the larger area is found to be concentration dependent. At higher NP concentrations, DPPG displays a kink region which is comparable to DPPC, except that the kink is observed at a surface pressure of approximately 30 mN m^{-1}, unlike DPPC (at approx. 25 mN m^{-1}). Again, a squeeze out of material could be observed at high NP concentrations.

3.2.4. Effect of nanoparticles on the isotherms of the mixed dipalmitoylphosphatidylcholine : dipalmitoylphophatidylglycerol monolayer. Since the effect of NPs on DPPC and DPPG is different when analysed individually, it was interesting to see the effect on the DPPC : DPPG mixture, which is the primary component of the LS model system. The surface pressure change of DPPC/DPPG (4 : 1 mol ratio) with a decrease in area per molecule is presented in figure 6*d*. The figure displays the change in the phase behaviour of lipid mixtures in the presence of increasing concentration of NPs. In the isotherms of the pure DPPC/DPPG mixture, it can be seen that DPPG is already having an influence on the phase behaviour of DPPC. The plateau region corresponding to le–lc phase coexistence has almost disappeared and shows an indistinct phase transition region. Adding NPs to the DPPC/DPPG mixture leads to a slight expansion of isotherms in a concentration-dependent manner. Similar to DPPC and DPPG, the lipid mixtures also exhibit a kink region at a surface pressure of approximately 25 mN m^{-1}, and, on further compression, the isotherm reaches a maximum with its slope shifting to a lower area per molecule compared with the slope of pure lipid mixture, on increasing NP concentration. Squeeze out of material is observed at a ratio of 5 : 1 and is even more pronounced at a ratio of 1 : 1.

3.2.5. Effect of nanoparticles on the isotherms of monolayers made of dipalmitoylphosphatidylcholine/dipalmitoylphophatidylglycerol and 0.4 mol% surfactant protein C. Figure 6*e* shows the pressure–area curves of the LS mimicking the mixture of DPPC/DPPG/SP-C. As already pointed out, the plateau area at 55 mN m^{-1} is nicely formed. Addition of NPs leads to a shift of the whole curve to lower areas and changes the slope of the plateau and shortens it (figure 6*f*, which is an enlargement of figure 6*e*). This clearly shows that NPs are incorporated into the lipid–peptide monolayer and that the typical structures shown in figures 1–3 are disturbed by the NPs, although the effect is less

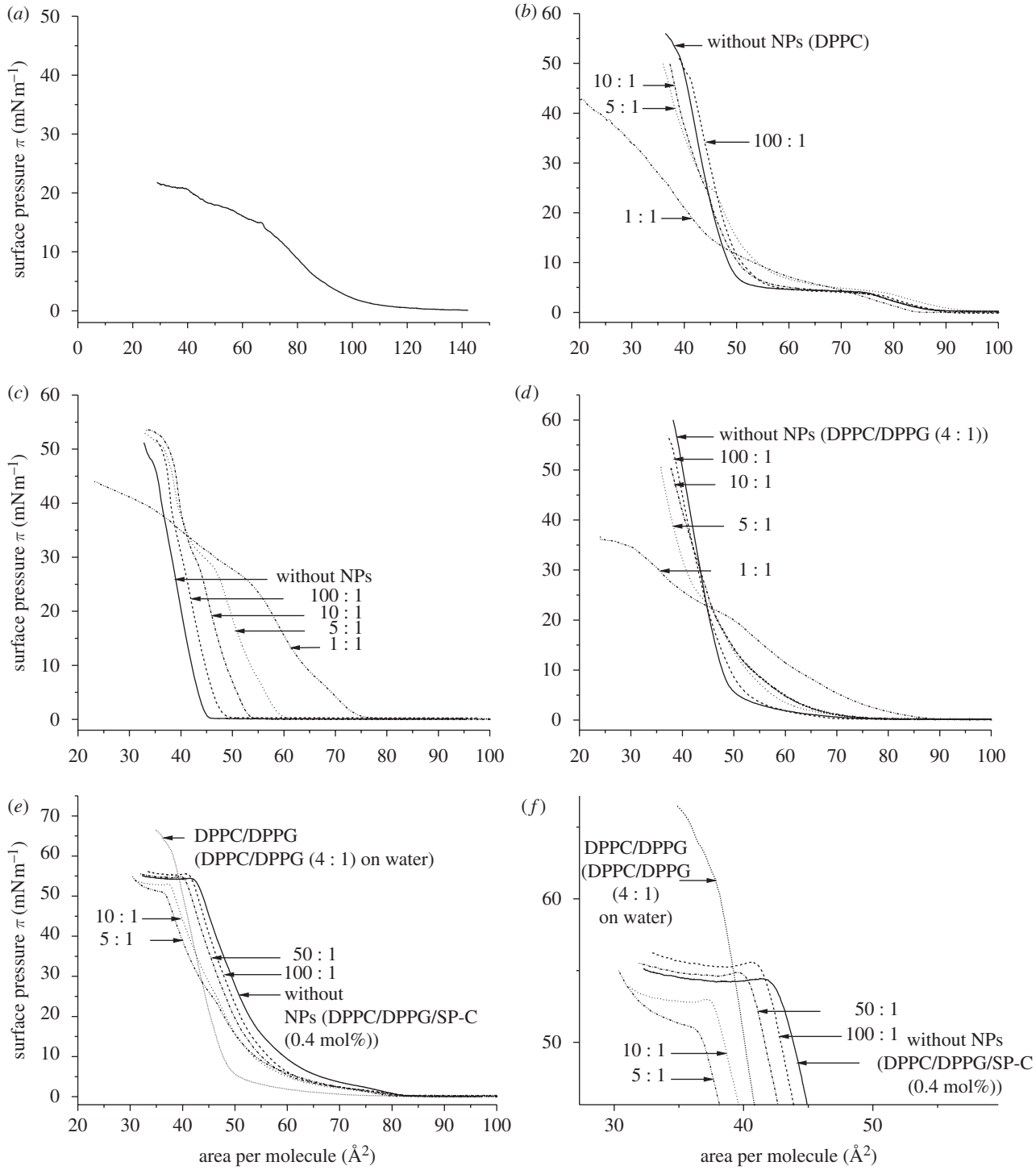

Figure 6. Surface pressure–area (π–A) isotherms of monolayer consisting of (*a*) pure AmorSil20 NPs (solid line), (*b*) DPPC, (*c*) DPPG, (*d*) DPPC/DPPG (4 : 1 mol ratio), (*e*,*f*) DPPC/DPPG/SPC (0.4 mol%) with different concentrations of AmorSil20 NPs. (*f*) An enlarged view of the plateau region from (*e*). All the measurements were performed on pure water (pH 5.6) at 20°C.

pronounced, as was observed in pure and mixed lipid films. However, an enhanced squeeze out is observed by the shift of the whole curve to lower areas and by the shift of the plateau to lower pressures.

3.3. Fluorescence microscopic studies

Fluorescence microscopy was performed to visualize the morphology of domain structures and to study the phase behaviour of the monolayer system on compression at a specific lateral surface pressure. Most importantly, it offers the opportunity to analyse the phase transition from le to lc phase. Every lipid or lipid–peptide mixture shows a difference in domain morphology providing basic information on the packing and orientation of constituent molecules within the monolayer. In this method, monolayers are doped with fluorescent probes and the domains are observed owing to the difference in their solubility within the lc or le region. The dyes cannot penetrate the tightly

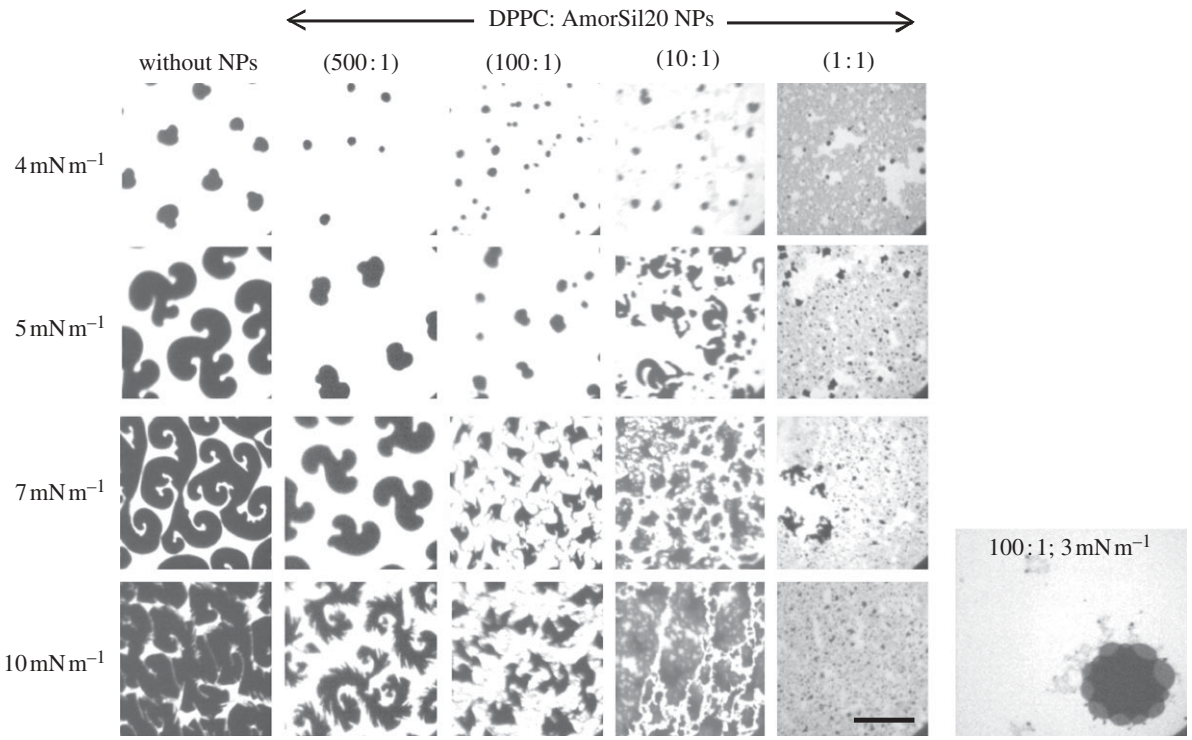

Figure 7. Fluorescence images of DPPC monolayer consisting of different concentrations of AmorSil20 NPs on pure water at 20°C. Images taken at different surface pressures are shown. An additional image showing the aggregates of NPs localized surrounding the rigid domains at the interface of the two phases. All samples were doped with 0.5 mol% fluorescent dye BODIPY-PC. Scale bar, 50 μm.

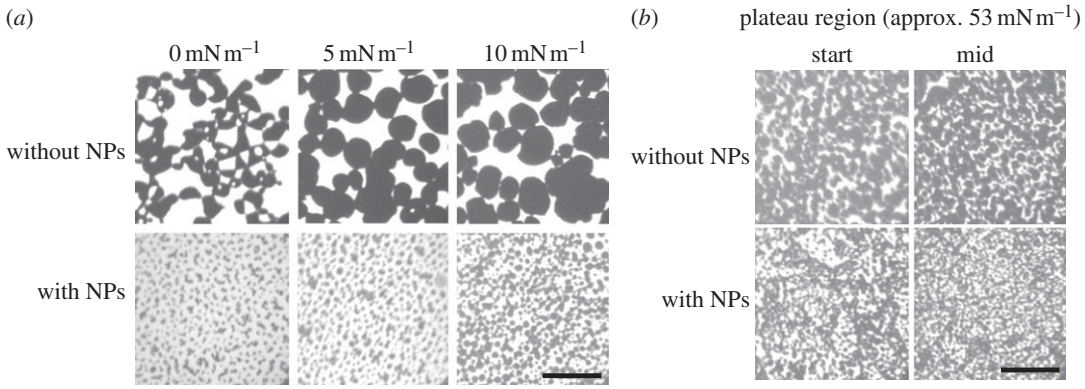

Figure 8. Fluorescence images of (*a*) DPPC/DPPG monolayer and (*b*) DPPC/DPPG/SP-C monolayer with and without AmorSil20 NPs (100 : 1) on pure water at 20°C. Images taken at different surface pressures are shown. All samples were doped with 0.5 mol% fluorescent dye BODIPY-PC. Scale bars, 50 μm.

packed lc region, and, therefore, preferentially localize in the le region owing to loosely packed lipid acyl chains. Hence, the rigid domain (lc) appears to be dark and is found embedded in the bright fluorescent fluid (le) background.

Here, for the first time, we present the fluorescent images of the DPPC monolayer containing NPs and study their effect on the morphology of DPPC domain shapes. In the past, several studies have been carried out examining pure DPPC domain structure formation with the le–lc phase-transition region (Klopfer & Vanderlick 1996; McConlogue & Vanderlick 1997). In this region, DPPC shows the kidney-shaped domain followed by a multi-lobed structure formation that disappears as it enters into the lc region forming a circular domain. Figure 7 shows a series of fluorescence microscopic images, captured at a specific surface pressure, of the DPPC monolayer containing different NP concentrations. The studies were conducted in a surface pressure range of 0–50 mN m^{-1}, but the main objective was to investigate the effect on the le–lc phase-transition region. Thus, only the fluorescence images at 4, 5, 7 and 10 mN m^{-1} are presented here. The phase-transition region starts at approximately 4 mN m^{-1} in the pure DPPC monolayer and thus the formation of the domain which is initially kidney shaped as observed in the images. Further compression of pure DPPC monolayers leads to nucleation

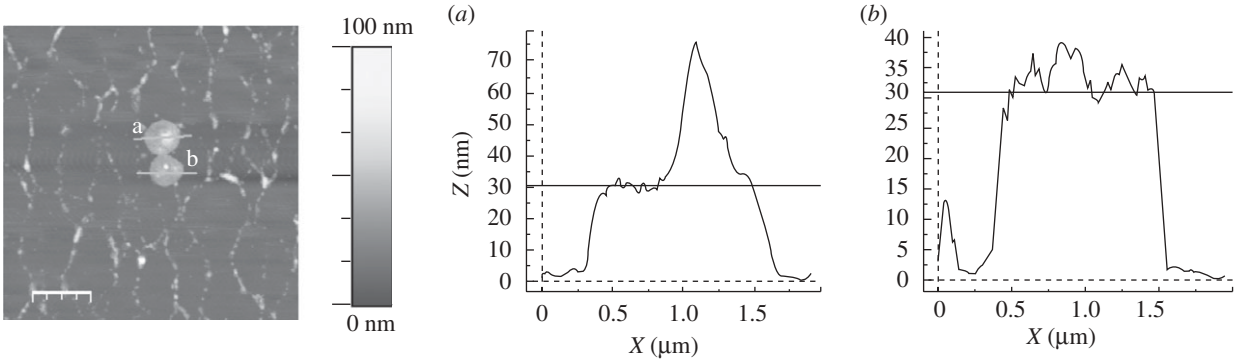

Figure 9. AFM topography images of a DPPC/DPPG/SP-C (0.4 mol%) monolayer consisting of AmorSil20 NPs (100 : 1 ratio). LB films were transferred onto mica at a surface pressure of approximately 53 mN m^{-1} from a subphase containing water (pH 5.6) at 20°C. All AFM images were taken in contact mode. Scan size is 10 × 10 μm^2. The height profiles (*a*,*b*) show the lateral dimension of the NP aggregates to be approximately 1 μm and the height to be approximately 30 nm. Scale bar, 20 μm.

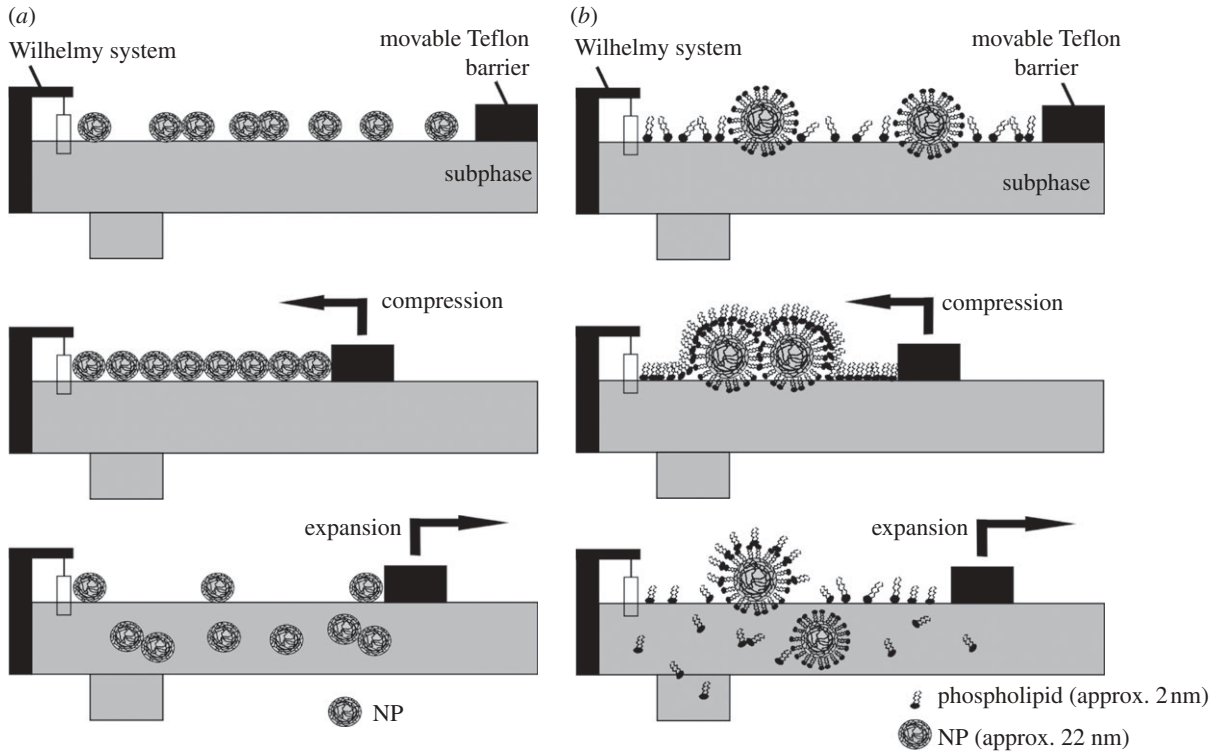

Figure 10. Schematic representation of the film balance measurement showing the potential interaction and the fate of molecules during the compression and expansion cycle. (*a*) Pure AmorSil20 NPs and (*b*) lipid–NP mixture.

and growth of domain size, forming multi-lobed structures, reaching a diameter of 80–100 μm at 10 mN m^{-1}. Addition of NPs to the DPPC monolayer delays the phase transition and hence the formation of the domain. At a low NP concentration (500 : 1), structures can still be observed but the process of nucleation of the domain is slowed and the diameter of the domain is decreased to 50–70 μm at 10 mN m^{-1}. The change in the shape and size of rigid domains depends on the opposing forces of line tension acting at the phase interface and the electrostatic interaction between the molecules within each domain (McConlogue & Vanderlick 1997; Hu *et al.* 2006; Garcia-Saez *et al.* 2007). It is probable that the aggregates of NPs found to be localized at the domain phase boundaries (additional picture in figure 7) have an influence on these delicate forces, thus preventing further nucleation and thereby inhibiting the increase in domain size. Hence, addition of NPs decreased the size of the rigid domain and expanded the surface area of the liquid phase in a concentration-dependent manner. No growth in domain size could be observed following their disappearance and irregular structures are formed.

The same is basically true for the DPPC/DPPG mixture. Again, the structures formed are strongly disturbed by the NPs already at a low concentration (100 : 1) (figure 8*a*). Inspection of the DPPC/DPPG/SP-C films by fluorescence in the plateau region showed that the typical domain structures observed

and characterized by different techniques (see above) are again disturbed by the addition of NPs (figure 8*b*).

3.4. Atomic force microscopy studies

AFM studies gave further hints on the interaction of the NPs with the surfactant mimicking monolayers. As shown in figure 9, clusters of NPs incorporate directly into the structural features discussed before as double-layer areas. The size of such an NP aggregate is about 1 μm; however, fine structures could be observed, fitting the size of single NPs. The overall structure is not changed; thus, we must conclude that the NPs are incorporated in the surfactant, covering themselves with lipids and/or proteins, and reducing the area as was demonstrated in figure 6*e*.

4. CONCLUSIONS AND PERSPECTIVES

We showed that organosiloxane NPs strongly interact with lipid monolayers representative of LS at the air–water interphase. The NPs strongly disturb the domain structure and thus the phase behaviour of the fluid and condensed domains and concentrate at the domain borders. NPs exhibit a characteristic preference for the rigid–fluid interface. We assume (figure 10) that the NPs cover themselves with lipids (Bakshi *et al.* 2008; Bothun 2008), thus becoming an integral part of the monolayer or the bilayer regions in the artificial surfactant film. Since under compression we are able to reach areas much lower than the area occupied by the corresponding lipid, we assume that the lipid-covered particles become covered with the remaining lipid monolayer. Owing to strong hysteresis effects, we have to consider the possibility that the lipid-covered NPs are able to escape into the water phase and thus in the alveolar system they will be able to cross the aqueous protein-containing hypophase to reach the cells in the alveolar wall. It would be interesting to see whether in the presence of proteins within the surfactant monolayer or the hypophase it will cover the NPs as well or in a mixture with lipids. This is an important point since just the pure NPs alone cannot account for the interaction with cells; rather more obviously, particles covered by lipids and/or proteins are more likely to be desirable for cellular interaction. We could also show that NPs had an effect on surfactant functioning during film compression and inhibited respreading during film expansion. This is in line with previous studies that demonstrated that the presence of NPs impedes surfactant adsorption and compression as well as the function of the surfactant proteins (Bakshi *et al.* 2008). In addition, the charge on the surfactant and/or NP could essentially influence the accretion of NPs on some crystal plane by preferentially enhancing crystal growth in an anisotropic manner (Bakshi *et al.* 2008). Together, all such implications might have a potential role in the onset of acute lung injury or acute respiratory distress syndrome (ARDS) (Nel *et al.* 2006; Wallace *et al.* 2007; Schleh & Hohlfeld 2009). Furthermore, it would be interesting to investigate the effect of NPs on adsorption of surface active materials from the subphase onto the surfactant monolayer at the air/water interface. Additionally, investigating NPs with different surface properties such as size and hydrophilicity with different surface charges would be interesting. The charges on the surface of the particles would differ in specificity in interaction with lipid and peptides influencing the shape and size of domains that would affect the surfactant function. In summary, our experiments clearly show that NPs interact with LS, slightly disturbing the surface structures and penetrating the surface layer to reach the alveolar cells.

This work is a contribution from the Schwerpunkt Programme SP1313 and was financially supported by the Deutsche Forschungsgemeinschaft (DFG). It was further subsidized by grants from our International Graduate School of Chemistry (to R.K.H. and M.S.). Finally, we would like to thank Tascon GmbH, Münster, Germany, especially Dr D. Breitenstein, for their continuous help with the TOF-SIMS experiments. Within the 'Bioneers' consortium, we like to thank Prof. J. Kirkpatrick and Prof. R. Stauber and Dr M. Maskos, University of Mainz, for helpful discussions. In addition, we thank Dr Maskos for making the NPs available to us.

REFERENCES

Amrein, M., von Nahmen, A. & Sieber, M. 1997 A scanning force- and fluorescence light microscopy study of the structure and function of a model pulmonary surfactant. *Eur. Biophys. J.* **26**, 349–357. (doi:10.1007/s002490050089)

Bakshi, M. S., Zhao, L., Smith, R., Possmayer, F. & Petersen, N. O. 2008 Metal nanoparticle pollutants interfere with pulmonary surfactant function *in vitro*. *Biophys. J.* **94**, 855–868. (doi:10.1529/biophysj.107.106971)

Bangham, A. D., Morley, C. J. & Phillips, M. C. 1979 The physical properties of an effective lung surfactant. *Biochim. Biophys. Acta* **573**, 552–556. (doi:10.1016/0005–2760(79)90229–7)

Benninghoven, A. 1994 Chemical analysis of inorganic and organic surfaces and thin films by static time-of-flight secondary ion mass spectrometry (TOF-SIMS). *Angewandte Chemie Int. Edn Eng.* **33**, 1023–1043. (doi:10.1002/anie.199410231)

Bothun, G. 2008 Hydrophobic silver nanoparticles trapped in lipid bilayers: size distribution, bilayer phase behavior, and optical properties. *J. Nanobiotechnol.* **6**, 13. (doi:10.1186/1477-3155-6-13)

Breitenstein, D., Batenburg, J. J., Hagenhoff, B. & Galla, H. J. 2006 Lipid specificity of surfactant protein B studied by time-of-flight secondary ion mass spectrometry. *Biophys. J.* **91**, 1347–1356. (doi:10.1529/biophysj.105.073247)

Clements, J. A. & Avery, M. E. 1998 Lung surfactant and neonatal respiratory distress syndrome. *Am. J. Respir. Crit. Care Med.* **157**, S59–S66.

Creuwels, L. A., van Golde, L. M. & Haagsman, H. P. 1997 The pulmonary surfactant system: biochemical and clinical aspects. *Lung* **175**, 1–39. (doi:10.1007/PL00007554)

Crouch, E. & Wright, J. R. 2001 Surfactant proteins a and d and pulmonary host defense. *Annu. Rev. Physiol.* **63**, 521–554. (doi:10.1146/annurev.physiol.63.1.521)

De Jong, W. H. & Borm, P. J. 2008 Drug delivery and nanoparticles: applications and hazards. *Int. J. Nanomed.* **3**, 133–149.

Dietl, P. & Haller, T. 2005 Exocytosis of lung surfactant: from the secretory vesicle to the air–liquid interface. *Annu. Rev. Physiol.* **67**, 595–621. (doi:10.1146/annurev.physiol.67.040403.102553)

Galla, H. J., Bourdos, N., von Nahmen, A., Amrein, M. & Sieber, M. 1998 The role of pulmonary surfactant protein C during the breathing cycle. *Thin Solid Films* **327–329**, 632–635. (doi:10.1016/S0040-6090(98)00728-7)

Garcia-Saez, A. J., Chiantia, S. & Schwille, P. 2007 Effect of line tension on the lateral organization of lipid membranes. *J. Biol. Chem.* **282**, 33 537–33 544. (doi:10.1074/jbc.M706162200)

Goerke, J. 1974 Lung surfactant. *Biochim. Biophys. Acta* **344**, 241–261. (doi:10.1016/0304-4157(74)90009-4)

Goerke, J. 1998 Pulmonary surfactant: functions and molecular composition. *Biochim. Biophys. Acta* **1408**, 79–89. (doi:10.1016/S0925-4439(98)00060-X)

Griese, M. 1999 Pulmonary surfactant in health and human lung diseases: state of the art. *Eur. Respir. J.* **13**, 1455–1476. (doi:10.1183/09031936.99.13614779)

Haagsman, H. P., Hawgood, S., Sargeant, T., Buckley, D., White, R. T., Drickamer, K. & Benson, B. J. 1987 The major lung surfactant protein, SP 28–36, is a calcium-dependent, carbohydrate-binding protein. *J. Biol. Chem.* **262**, 13877–13880.

Hills, B. A. 1990 The role of lung surfactant. *Br. J. Anaesth.* **65**, 13–29.

Hoet, P. H., Bruske-Hohlfeld, I. & Salata, O. V. 2004 Nanoparticles—known and unknown health risks. *J. Nanobiotechnol.* **2**, 12. (doi:10.1186/1477-3155-2-12)

Horcas, I., Fernandez, R., Gomez-Rodriguez, J. M., Colchero, J., Gomez-Herrero, J. & Baro, A. M. 2007 WSXM: a software for scanning probe microscopy and a tool for nanotechnology. *Rev. Sci. Instrum.* **78**, 013705–013708. (doi:10.1063/1.2432410)

Hu, Y., Meleson, K. & Israelachvili, J. 2006 Thermodynamic equilibrium of domains in a two-component Langmuir monolayer. *Biophys. J.* **91**, 444–453. (doi:10.1529/biophysj.106.081000)

Kishore, U. *et al.* 2006 Surfactant proteins SP-A and SP-D: structure, function and receptors. *Mol. Immunol.* **43**, 1293–1315. (doi:10.1016/j.molimm.2005.08.004)

Klopfer, K. J. & Vanderlick, T. K. 1996 Isotherms of dipalmitoylphosphatidylcholine (DPPC) monolayers: features revealed and features obscured. *J. Colloid Interface Sci.* **182**, 220–229. (doi:10.1006/jcis.1996.0454)

Krol, S., Janshoff, A., Ross, M. & Galla, J. 2000*a* Structure and function of surfactant protein B and C in lipid monolayers: a scanning force microscopy study. *Phys. Chem. Phys.* **2**, 4586–4593. (doi:10.1039/b004145i)

Krol, S., Ross, M., Sieber, M., Kunneke, S., Galla, H. J. & Janshoff, A. 2000*b* Formation of three-dimensional protein-lipid aggregates in monolayer films induced by surfactant protein B. *Biophys. J.* **79**, 904–918. (doi:10.1016/S0006-3495(00)76346-6)

Ku, T., Gill, S., Lobenberg, R., Azarmi, S., Roa, W. & Prenner, E. J. 2008 Size dependent interactions of nanoparticles with lung surfactant model systems and the significant impact on surface potential. *J. Nanosci. Nanotechnol.* **8**, 2971–2978. (doi:10.1166/jnn.2008.171)

Malcharek, S., Hinz, A., Hilterhaus, L. & Galla, H. J. 2005 Multilayer structures in lipid monolayer films containing surfactant protein C: effects of cholesterol and POPE. *Biophys. J.* **88**, 2638–2649. (doi:10.1529/biophysj.104.050823)

Mazzola, L. 2003 Commercializing nanotechnology. *Nat. Biotechnol.* **21**, 1137–1143. (doi:10.1038/nbt1003-1137)

McConlogue, C. W. & Vanderlick, T. K. 1997 A close look at domain formation in DPPC monolayers. *Langmuir* **13**, 7158–7164. (doi:10.1021/la970898e)

Nel, A., Xia, T., Madler, L. & Li, N. 2006 Toxic potential of materials at the nanolevel. *Science* **311**, 622–627. (doi:10.1126/science.1114397)

Oosterlaken-Dijksterhuis, M. A., Haagsman, H. P., van Golde, L. M. & Demel, R. A. 1991*a* Characterization of lipid insertion into monomolecular layers mediated by lung surfactant proteins SP-B and SP-C. *Biochemistry* **30**, 10 965–10 971. (doi:10.1021/bi00109a022)

Oosterlaken-Dijksterhuis, M. A., Haagsman, H. P., van Golde, L. M. & Demel, R. A. 1991*b* Interaction of lipid vesicles with monomolecular layers containing lung surfactant proteins SP-B or SP-C. *Biochemistry* **30**, 8276–8281. (doi:10.1021/bi00247a024)

Pastrana-Rios, B., Flach, C. R., Brauner, J. W., Mautone, A. J. & Mendelsohn, R. 1994 A direct test of the 'squeeze-out' hypothesis of lung surfactant function. External reflection FT-IR at the air/water interface. *Biochemistry* **33**, 5121–5127. (doi:10.1021/bi00183a016)

Perez-Gil, J. 2008 Structure of pulmonary surfactant membranes and films: the role of proteins and lipid–protein interactions. *Biochim. Biophys. Acta* **1778**, 1676–1695. (doi:10.1016/j.bbamem.2008.05.003)

Reid, K. B. 1998 Functional roles of the lung surfactant proteins SP-A and SP-D in innate immunity. *Immunobiology* **199**, 200–207.

Roos, C., Schmidt, M., Ebenhoch, J., Baumann, F., Deubzer, B. & Weis, J. 1999 Design and synthesis of molecular reactors for the preparation of topologically trapped gold cluster. *Adv. Mater.* **11**, 761–766. (doi:10.1002/(SICI)1521-4095(199906)11:9<761::AID-ADMA761>3.0.CO;2-D)

Ross, M., Krol, S., Janshoff, A. & Galla, H. J. 2002 Kinetics of phospholipid insertion into monolayers containing the lung surfactant proteins SP-B or SP-C. *Eur. Biophys. J.* **31**, 52–61. (doi:10.1007/s002490100181)

Salata, O. 2004 Applications of nanoparticles in biology and medicine. *J. Nanobiotechnol.* **2**, 3. (doi:10.1186/1477-3155-2-3)

Saleem, M., Meyer, M. C., Breitenstein, D. & Galla, H. J. 2008 The surfactant peptide KL4 in lipid monolayers: phase behavior, topography, and chemical distribution. *J. Biol. Chem.* **283**, 5195–5207. (doi:10.1074/jbc.M705944200)

Saleem, M., Meyer, M. C., Breitenstein, D. & Galla, H. J. 2009 Calcium ions as 'miscibility switch': colocalization of surfactant protein B with anionic lipids under absolute calcium free conditions. *Biophys. J.* **97**, 500–508. (doi:10.1016/j.bpj.2009.05.011)

Schleh, C. & Hohlfeld, J. M. 2009 Interaction of nanoparticles with the pulmonary surfactant system. *Inhal. Toxicol.* **21**, 97–103. (doi:10.1080/08958370903005744)

Schurch, S., Goerke, J. & Clements, J. A. 1976 Direct determination of surface tension in the lung. *Proc. Natl Acad. Sci. USA* **73**, 4698–4702. (doi:10.1073/pnas.73.12.4698)

Schurch, S., Qanbar, R., Bachofen, H. & Possmayer, F. 1995 The surface-associated surfactant reservoir in the alveolar lining. *Biol. Neonate* **67**(Suppl. 1), 61–76.

Seifert, M., Breitenstein, D., Klenz, U., Meyer, M. C. & Galla, H. J. 2007 Solubility versus electrostatics: what determines lipid/protein interaction in lung surfactant. *Biophys. J.* **93**, 1192–1203. (doi:10.1529/biophysj.107.106765)

Stuart, D., Löbenberg, R., Ku, T., Azarmi, S., Ely, L., Roa, W. & Prenner, E. J. 2006 Biophysical investigation of nanoparticle interactions with lung surfactant model

systems. *J. Biomed. Nanotechnol.* **2**, 245–252. (doi:10.1166/jbn.2006.031)

Sung, J. C., Pulliam, B. L. & Edwards, D. A. 2007 Nanoparticles for drug delivery to the lungs. *Trends Biotechnol.* **25**, 563–570. (doi:10.1016/j.tibtech.2007.09.005)

Taneva, S. G., Stewart, J., Taylor, L. & Keough, K. M. 1998 Method of purification affects some interfacial properties of pulmonary surfactant proteins B and C and their mixtures with dipalmitoylphosphatidylcholine. *Biochim. Biophys. Acta* **1370**, 138–150. (doi:10.1016/S0005-2736(97)00257-5)

Veldhuizen, R., Nag, K., Orgeig, S. & Possmayer, F. 1998 The role of lipids in pulmonary surfactant. *Biochim. Biophys. Acta* **1408**, 90–108. (doi:10.1016/S0925-4439(98)00061-1)

von Nahmen, A., Schenk, M., Sieber, M. & Amrein, M. 1997 The structure of a model pulmonary surfactant as revealed by scanning force microscopy. *Biophys. J.* **72**, 463–469. (doi:10.1016/S0006-3495(97)78687-9)

Wallace, W., Keane, M., Murray, D., Chisholm, W., Maynard, A. & Ong, T.-M. 2007 Phospholipid lung surfactant and nanoparticle surface toxicity: Lessons from diesel soots and silicate dusts. *J. Nanoparticle Res.* **9**, 23–38. (doi:10.1007/s11051-006-9159-5)

Watkins, J. C. 1968 The surface properties of pure phospholipids in relation to those of lung extracts. *Biochim. Biophys. Acta* **152**, 293–306. (doi:10.1016/0005-2760(68)90037-4)

Yang, W., Peters, J. I. & Williams 3rd, R. O. 2008 Inhaled nanoparticles—a current review. *Int. J. Pharm.* **356**, 239–247. (doi:10.1016/j.ijpharm.2008.02.011)

Yu, S., Harding, P. G., Smith, N. & Possmayer, F. 1983 Bovine pulmonary surfactant: chemical composition and physical properties. *Lipids* **18**, 522–529. (doi:10.1007/BF02535391)